FEATURE ARTICLE

ChemComm
www.rsc.org/chemcomm

Electrostatic interactions by design. Versatile methodology towards multifunctional assemblies/nanostructured electrodes

Dirk M. Guldi[a,b] and Maurizio Prato[c]

[a] *Universität Erlangen, Institute for Physical Chemistry, 91058 Erlangen, Germany*
[b] *University of Notre Dame, Radiation Laboratory, Notre Dame, IN 46556, USA*
[c] *Dipartimento di Scienze Farmaceutiche, Università di Trieste, Piazzale Europa 1, Trieste 34127, Italy*

Received (in Cambridge, UK) 9th July 2004, Accepted 13th September 2004
First published as an Advance Article on the web 27th October 2004

This *Feature Article* describes how multi-site interactions between positively or negatively charged carbon forms, such as fullerenes and single wall carbon nanotubes, and porphyrinic chromophores have been utilized *en route* towards novel multifunctional and nanostructured materials. Specifically, we discuss (*i*) the behavior of molecular assemblies in homogeneous solutions and (*ii*) the controlled self-assembly on surfaces.

One of the key challenges in devising multifunctional assemblies and/or nanostructured surfaces is the tailoring of materials by adequately chosen assembly methods, which control electronic structures and enhance desired functionalities.[1] To associate multicomponent assemblies, which should be thermodynamically stable and robust, a fine-tuned interplay of interactions at the nanoscale level is necessary. An important structural aspect is that the configuration of the resulting assemblies is determined by the chemical information encoded into the individual building blocks and the specific arrangement of the binding sites.

Based on its universality and widespread use in biological systems, electrostatic complexation emerges as a *simple*, but also *powerful* approach.[2] Such a methodology towards functional and nanometer-scale systems guarantees efficient bindings both in homogeneous (*i.e.*, condensed media) and in heterogeneous (*i.e.*, interfaces) environments. In addition, it offers control over the molecularly organized integration of functional building blocks and the performance of the required function.

A particularly strong driving force for applications of this technique is the use of new multifunctional materials within the context of light-induced charge separation and solar-energy conversion.[3] This approach holds great promise to build on innovative and unique routes to design novel nanoscale materials as viable tools to improve the performance in model energy conversion. The integration of complementary motifs, that is, several positively and negatively charged binding sites in combination with van der Waals or other weak interactions expands the possible scope of this technique.

One set of active components in the nanostructures considered in this article are positively or negatively charged carbon forms, such as fullerenes[4]—in particular C_{60}—and single wall carbon nanotubes[5] (SWNT). Implementation of C_{60} as a three dimensional electron acceptor has been widely explored on account of its small reorganization energy in electron transfer reactions and has exerted noteworthy impact on the improvement of light-induced charge-separation.[6] The complementary class of materials for alternate electrostatic depositions is based on different charged porphyrin macrocyclic skeletons.[7] In fact, fullerenes and porphyrins (*i.e.*, either zinc tetraphenylporphyrin, ZnP, or free base tetraphenylporphyrin, H_2P) are ideally suited for devising integrated, multicomponent model systems to transmit and process solar energy.

Several powerful methodologies have been developed that allow the chemical functionalization of fullerenes in simple or even sophisticated ways.[4] Based on these methods, the synthesis of relatively complex molecular architectures—tetrads and even hexads—has been accomplished. Particularly promising results have been obtained with efficient charge-separation processes ($\sim$30%) within molecular assemblies of nanometer dimensions (*i.e.*, Fc–ZnP–H_2P–C_{60} and Fc–ZnP–ZnP–C_{60}).[8] More outstandingly, the lifetime of the spatially-separated ($\sim$50 Å) radical pair, product of a sequence of energy and electron transfer steps, reaches into a time domain (*i.e.*, seconds) hardly accomplished so far in artificial photosynthesis.

However, owing to the multi-step and complex synthetic procedure, the necessity for simpler systems arises. One potent approach implies organization principles, such as biomimetic methodologies, that help regulate size, shape and function down to the molecular scale.[2] Hydrogen-bonding, π–π stacking,

Dirk M. Guldi graduated from the University of Cologne (Germany) in 1988, from where he received his PhD in 1990. In 1992, after a postdoctoral appointment at the National Institute of Standards and Technology, he took a research position at the Hahn-Meitner-Institute Berlin. After a brief stay as a Feodor-Lynen Stipend (Alexander von Humboldt Foundation) at Syracuse University he joined in 1995 the faculty of the Notre Dame Radiation Laboratory where he was promoted to Associate Scientist in 1996. In 1999 he completed his Habilitation at the University of Leipzig (Germany). Since 2004 he has been Professor of Physical Chemistry at the Friedrich-Alexander University in Erlangen (Germany). He was awarded the Heisenberg-Prize (1999; Deutsche Forschungsgemeinschaft), Grammaticakis-Neumann-Prize (2000; Swiss Society for Photochemistry and Photophysics), JSPS Fellowship (2003; The Japan Society for the Promotion of Science and JPP-Award (2004; Society of Porphyrins and Phthalocyanines). His primary research interests are in the areas of new multifunctional carbon-based nanostructures within the context of light-induced charge separation and solar-energy conversion.

Maurizio Prato is Professor of Organic Chemistry in the Faculty of Pharmacy at the University of Trieste. He studied Chemistry at the University of Padova, where he became Assistant Professor in 1983. Then he moved to Trieste in 1992 as Associate Professor. After spending a postdoctoral period in 1986–87 at Yale University with S. J. Danishefsky, he was Visiting Scientist in 1992–93 at the University of California, Santa Barbara, working with F. Wudl. He was also Professeur Invité at the Ecole Normale Supérieure in Paris, France, in June–July 2002. His research focuses on the functionalization chemistry of fullerenes and carbon nanotubes for applications in materials science and medicinal chemistry, and on the synthesis of biologically active substances. His scientific contributions have been recognized by National awards including: the Federchimica Prize (1995, Association of Italian Industries), the National Prize for Research (2002, Italian Chemical Society), and an Honor Mention from the University of Trieste in 2004.

DOI: 10.1039/b410541a

metal-mediated complexation, and electrostatic interactions may promote engineering of elaborated and complex architectures. This supramolecular approach guarantees a greater control over the organization and an increased flexibility in replacing individual building blocks.

The major thrust of this article is to illustrate the versatility of designing multi-site interactions between proper components. Their potential for materials processing and molecular engineering into layered nanostructured materials is outlined. Our strategy consists of assembling well-defined molecular architectures: we start with building blocks (*i.e.*, at an atomic and/or molecular scale) that gives access to *a priori* design of multifunctional molecular materials and their assembly into two/three-dimensional solid nanostructures. In addition, interfacially assembled or organized architectures and layer-by-layer (LBL) films are surveyed that are directed by electrostatic and van der Waals interactions.[9]

In the first part, we will examine the behavior of the molecular assemblies in homogeneous solutions. This introductory section will be followed by considerations related to the controlled self-assembly on surfaces.

To harvest the full potential of electrostatic complexations, only truly water-soluble building blocks (*i.e.*, sensitizer molecules, soluble carbon nanostructures, and semiconductor nanoparticles) are considered. Water solubility provides flexibility, such as pH variation and ionic strength that may affect the interactions.

Of the system considered, water-soluble systems **1**/**2**[10] and **3**—shown in Figs. 1–3 contain only a single or two addends covalently attached to the C_{60} core. In mono- and bisadducts of C_{60} the characteristic electron acceptor behavior of the parent system is mostly retained, while in higher adducts, such as hexakisadducts, significant alterations of the fullerene character occur.[11] Methylation of the nitrogen atom in fulleropyrrolidines increases the electron acceptor character—see **3**.[12] At pH $\approx$ 7 the dendritic fullerene systems **1** and **2** are highly ionized, with a negative charge of 8 per each branch.

The dendritic fullerene oligocarboxylate **1** and the octapyridinium zinc porphyrin salt ZnP self-associate in water solution to form a 1 : 1 complex, with the remarkably high association constant of $3.5 \pm 1.0 \times 10^8$ M^{-1}.[13] Upon light irradiation, intermolecular electron transfer occurs, with the relatively long lifetime of 1.1 μs for the charge-separated state.

The topological parameters of the ZnP–**1** complex were calculated by molecular dynamic (MD) simulations, which give a π–π distance of about 8 Å. MD studies also show that **1** is not able to completely cover ZnP, but leaves approximately half of the molecule exposed, which, in principle, could be used to electrostatically attach other charged chromophores.

The polycharged ZnP can therefore be considered as an example for the electrostatically driven hybridization of polycationic redox species. In fact, this very general concept can be easily extended to biologically important proteins. Mitochondrial cytochrome *c* (Cyt*c*) is a polycationic redox protein, which serves as a mediator for electron transfer processes in biological systems. In Cyt*c* a net charge of 8 at pH 7 provides efficient coupling with oppositely charged entities, similar to the previously discussed ZnP. Pronounced electrostatic interactions between the positively

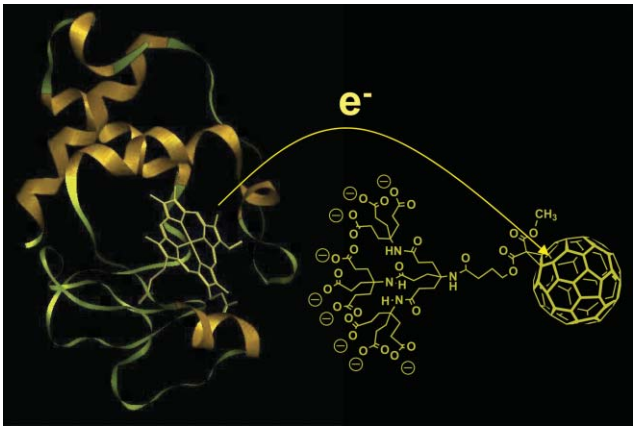

Fig. 2 Schematic representation of ZnCyt*c*–**1** binding and intracomplex electron transfer from the photoexcited ZnCyt*c* to the electron accepting fullerene.

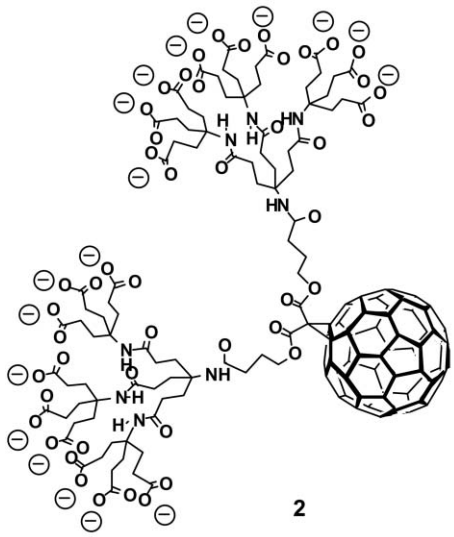

Fig. 3 Structure of fullerene derivative **2**.

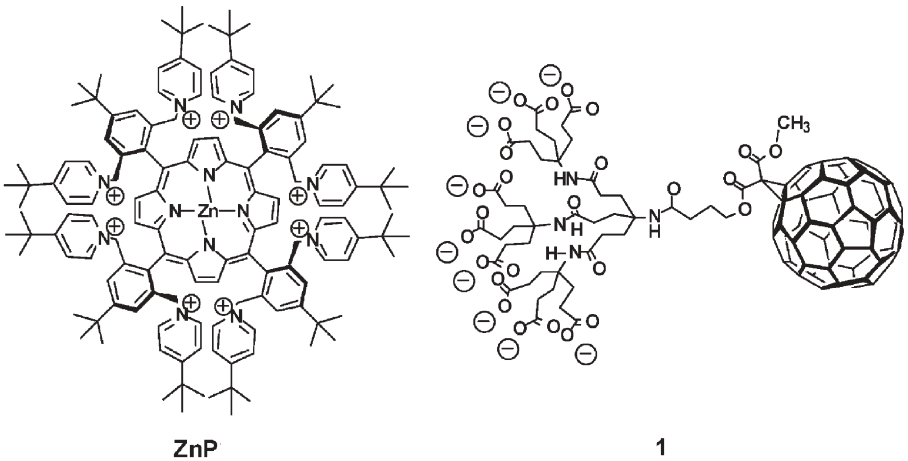

Fig. 1 Dendrimer fullerene polyelectrolyte **1** and octakis(pyridinium) zinc porphyrin ZnP.

charged ZnCyt*c* and the polyanionic dendrofullerenes **1** and **2** lead to the formation of stable protein–fullerene hybrids.[14] Both the dendrofullerenes and the protein contain redox active chromophores, which can be used as reporter moieties for the detection of hybridization and subsequent electronic interactions within the complexes. Fluorescent measurements revealed 1 : 1 hybrids ZnCyt*c*–**1** and ZnCyt*c*–**2** when using a large excess of **1** or **2**. The association constants were determined in the range of 10^5 M^{-1}. The coupling to **1** and **2** causes fluorescence quenching of the porphyrin emission within ZnCyt*c*. The reason for the fluorescence quenching is a photoinduced electron-transfer between the redox protein and the fullerene chromophore.

The interactions between ZnCyt*c* and **1/2** are affected by pH and ionic strength of the medium, which control the number of protonated/deprotonated carboxylate groups of **1/2**. This new hybridization concept of proteins, using the fullerene chromophore as a reporter unit, has a large potential for the investigation of electronic and functional properties of a broad range of charged proteins. Moreover, the discovery of very strong electrostatic interactions between the protein and the charged dendrimers can be used for the self-assembly of molecular electronic devices (*vide infra*).

Single wall carbon nanotubes (SWNT)[5] also serve as electron acceptor components in donor–acceptor assemblies, just as fullerenes have been the electron acceptors in much recent research.[15] Notably, the expected electrical conductivity behavior associated with the tubular structure and good chemical stability opens new promising scenarios for their use as "molecular wires" with high surface areas in the design of electro- and photoactive assemblies. We recently succeeded in testing the coulomb complex formation of water-soluble SWNT grafted with poly(sodium 4-styrenesulfonate) (SWNT-PSS)[16] and a zinc complex of 5,10,15,20-tetrakis-(2′,6′-bis-(*N*-methylene-(4″-*tert*-butylpyridinium))-4′-*tert*-butylphenyl)porphyrin octabromide salt (ZnP) *en route* to versatile donor–acceptor nanohybrids—see Fig. 4.[17] Photoexcitation of the porphyrin chromophore is followed by a rapid and efficient intra-ensemble charge separation to generate an ion-pair state that lives for tens of microseconds.

The use of electrostatic interactions can also be applied *en route* towards novel organic/inorganic mixed-nanocomposites, which prove to be promising in the context of solar energy conversion and photovoltaic reactivity.[18] For example, interactions of positively charged C_{60} derivatives, such as **3**, with three different size-quantized CdTe nanoparticles (NP)—see Fig. 5—led to novel organic (fullerene)–inorganic (NP) donor–acceptor hybrids. In particular, green (2.4 nm), yellow (3.4 nm), and red (5.0 nm) NP were examined, carrying either L-cysteine or thioglycolic acid as surface stabilizers. Fairly strong complexes were formed in these assemblies, for which association constants of $1 \pm 0.5 \times 10^5$ M^{-1} were determined in excess of NP. The electrostatic binding of **3** to NP facilitates a rapid intracomplex charge injection of a conduction band electron of the photoexcited NP to the surface-bound **3**. In the presence of **3**, when forming NP–**3**, the photoexcited NP transform nearly instantaneously into a charge-separated radical ion-pair. The radical ion-pair is remarkably stable throughout the timescale of up to several hundred microseconds from which a lifetime of 1.5 ± 0.5 ms (!) was determined. Also visible changes in the morphology, as seen in transmission electron microscopy (TEM), evolve from the strong association constants. TEM images of red NP ($\sim 10^{-5}$ M) alone are characteristic of uniformly shaped spheres, with a mean diameter of 6 ± 1 nm. In the case of the NP–**3** composite (*i.e.*, 10^{-5} M NP and 10^{-4} M **3**), a clearly different nanometer-sized pattern is seen, which can be attributed to electrostatically driven aggregation of NP and **3**. For example, nanometer-sized pattern of larger objects—with higher density of electrons—are derived for NP–**3** composite from the TEM image shown in the insert to Fig. 5. These results open new exciting possibilities for further transferring and engineering of these redox processes at the electrodes.

In fact, the scope of a more practical function of electrostatic interactions is to build mixed composite thin films, whose intrinsic nanonetworks can lead to significant improvements in energy conversion and transport. Solid thin films for use in photovoltaics can be prepared in many ways. Here we describe two different approaches that have been successfully applied in our laboratories.

Langmuir films[19]

A floating layer of amphiphilic, cationic **4** was deposited at the air–water interface.[20] Hereby, the hydrophilic functionality of **4**, an oligoethylene glycol chain with an ammonium end group, is immersed into the aqueous subphase. Fig. 6 illustrates the polyanionic, water-soluble porphyrin derivative (*i.e.*, H_2TPPPO(OH)$_2$–**5**), which is placed into the aqueous subphase, where the ammonium termini in **4** function as discrete and weakly interacting groups. A variety of techniques (*i.e.*, Langmuir isotherms, Brewster Angle Microscopy and UV-Vis Reflection Spectroscopy) confirmed the effective interactions between the two moieties at the air–water interface. Transfer of **4**–**5** *via* horizontal lifting, better known as the Langmuir–Shäfer method (LS), to several substrates allowed the fabrication of high quality, robust and photoactive films.

The characterization of the LS films by UV-Vis spectroscopy revealed that the two components behave as discrete and weakly

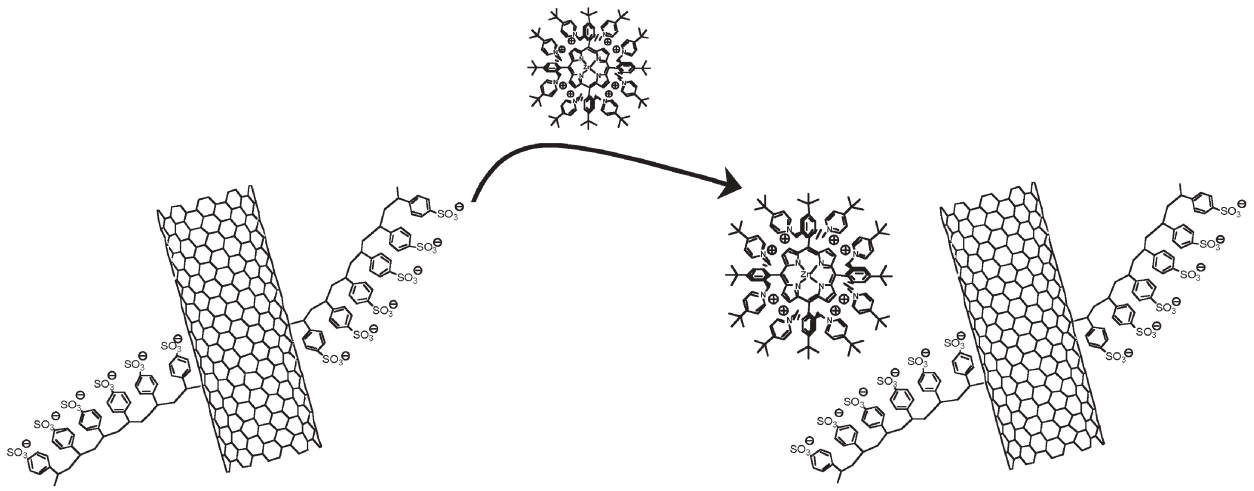

Fig. 4 Schematic representation of SWNT-PSS–ZnP formation.

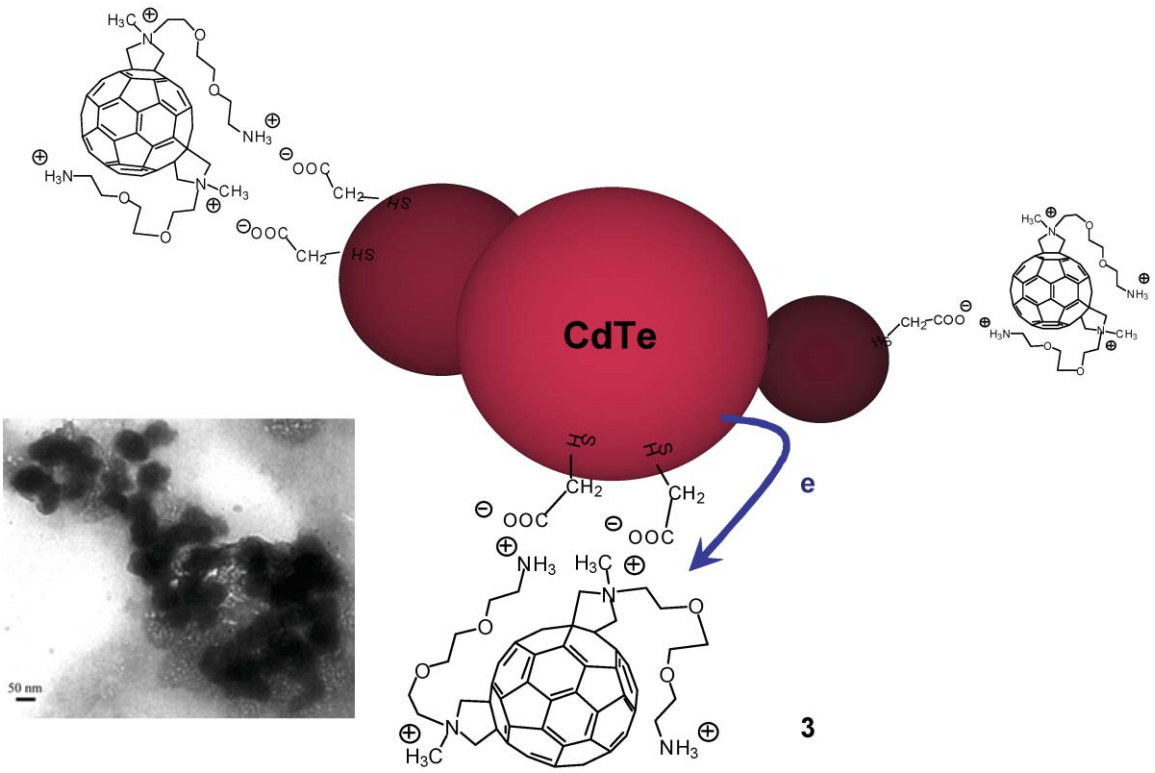

Fig. 5 Schematics for the spontaneous association of CdTe nanoparticles (NP) with **3**. Insert displays a TEM image of NP–**3**.

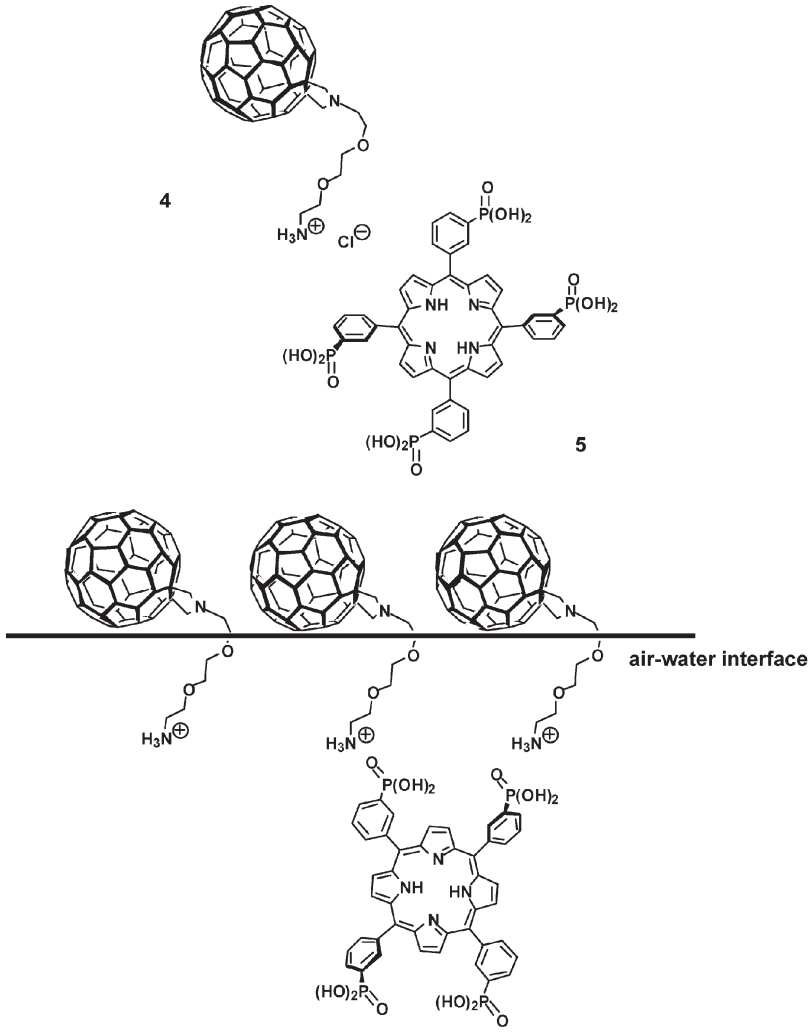

Fig. 6 Structure of fullerene derivative **4** and $H_2TPPPO(OH)_2$ **5**—upper part. Formation of **4**–**5** at the air–water interface—lower part.

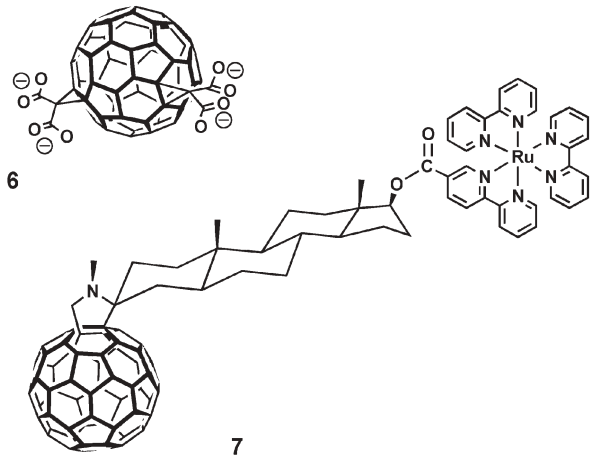

Fig. 7 Structures of **6** and **7**.

interacting π-systems. The use of polarized light suggested the existence of a preferential direction of macrocycle rings in **4–5** with an edge-on arrangement relative to the substrate surface. Finally, photoaction spectra were taken from films deposited by only one horizontal lifting sequence but at different surface pressures onto ITO electrodes. The observed photocurrents increased notably with increasing transfer surface pressure.

Important is that only through a correct balance of the hydrophobic and hydrophilic parts in C_{60} derivatives high quality monolayers are formed. Preparation of Langmuir Blodgett films (LB) from these intriguing species, deposited on the surface of appropriate electrodes, permits the viable construction of ultrathin modified electrodes with a high density of electroactive sites for their application as sensors, photoelectrochemical devices or photoelectrochemical information storage devices.

Layer-by-layer deposition[9]

The successful modification of solid-condensed interfaces, including photoactive ITO-electrodes, was accomplished based on the LBL approach. The strategy, employing donor–acceptor assemblies—covalently linked or noncovalently associated—bearing multiply charged functionalities, provides numerous advantages. Most importantly, the control over both the layer sequence and composition of the sandwich-like structures can be utilized for fine-tuning the electronic properties of the nanostructures. Despite some limitations imposed by the interpenetration of the adjacent layers, this method constitutes a potent alternative to traditional thin film techniques in fabricating photoactive molecular devices due to its simplicity and universality combined with high quality of LBL films.

Initial studies on LBL multilayered stacks of fullerene derivatives (*i.e.*, *e*-$C_{60}[C(COO^{-})_2]_2$–**6**) and fullerene-based donor–acceptor assemblies (*i.e.*, ruthenium(II) polypyridyl-C_{60}–**7**) gave access to densely packed, highly ordered films and stacks.[21] Among the many assets of such films and/or stacks especially promising are the energy conversion characteristics, namely, high photoactivity combined with environmental stability.

The substrates used in these studies were glass, quartz or indium tin oxide (ITO). Initially, a base layer of poly-(diallyl-dimethyl-ammonium)—PDDA—was deposited onto the hydrophobic surfaces *via* simple hydrophobic–hydrophobic interactions (step 1). The resulting hydrophilic and positively-charged surface promotes the electrostatically driven deposition of poly-(sodium-4-styrene-sulfonato)—PSS—(step 2), bearing sulfonic acid functionalities, to yield PDDA/PSS templates. For example, charge attraction is operative between the negative sulfonate groups in PSS and the pyrrolidinium cation in PDDA. Now that the surface is sufficiently overlaid with negative charges, key molecules such as **7** can be deposited by immersing the substrates into a dichloromethane/acetonitrile (1 : 1 *v*/*v*) solution of **7** (step 3). Fig. 8 summarizes the sequence of steps 1–3. Uniformly directed coulombic forces and short-range van der Waals forces govern the physisorption process between PSS and **7**. Sequential repetition of steps 2 and 3, that is, deposition of PSS and **7** allows the systematic stacking of PSS/**7** sandwich layers. Simpler is the deposition of **6** through the direct deposition onto PDDA. Subsequent sandwich units were assembled by repeating the alternating immersion of the substrates into aqueous solutions of PDDA and/or of **6** several times to produce films consisting of sandwich units.

It is important to note that after linking **6** or **7** to the base layer a hydrophobic surface is created, due to the presence of the fullerene moieties. Associative forces such as van der Waals interactions, which typically govern the connection between individual fullerene entities, is then believed to be the driving force for the 1-dimensional controlled build-up of another monolayer of **6** or **7** onto this hydrophobic surface. Evidence for the uniform packing was obtained from absorption spectra taken after each deposition increment. The linearity of the plot of the absorbance *versus* the number of layers indicated the uniformity of the sandwich units. Surface plasmon spectroscopy provided another convenient means for monitoring the thickness regularities of the built-up of the films. The assembly of each layer results in the gradual shift of the surface plasmon curve to a higher degree, indicating a greater thickness. The adsorption of **6** or **7** typically decreased the roughness of the surface, while fine-grained structures of the fullerene layer appeared. In particular, the surface becomes uniformly covered with characteristic 2D aggregates, of 20–50 nm size. Under

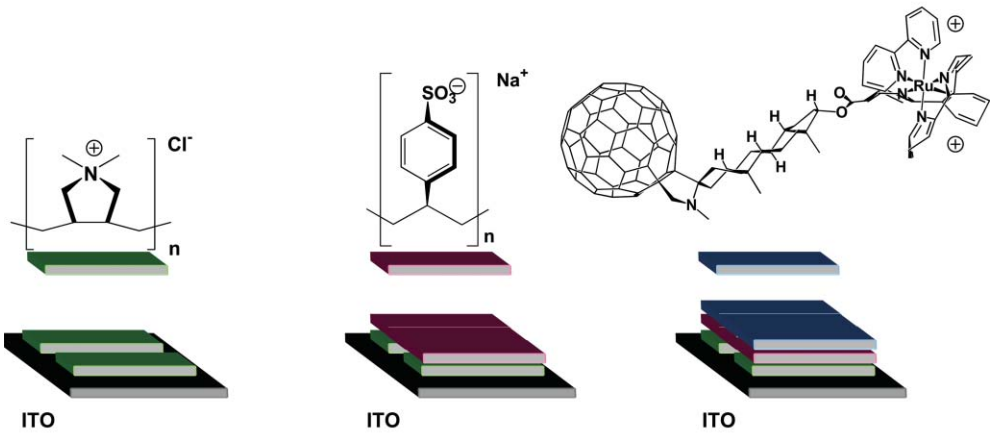

Fig. 8 Individual LBL steps for the deposition of PDDA (step 1—left), PSS (step 2—center) and **7** (step 3—right)—see text for details.

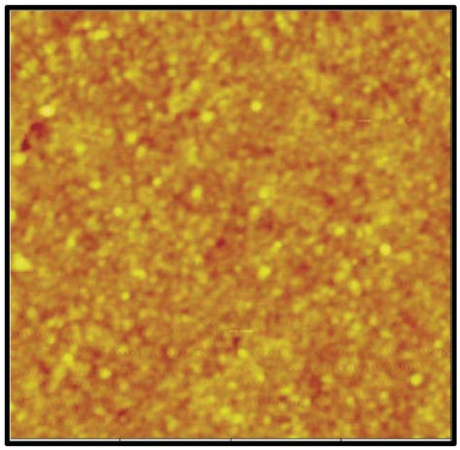

Fig. 9 Atomic force microscopy image of PDDA/PSS/7 assembled onto a cleaned silicon wafer—scale is 1 μm × 1 μm.

optimized deposition conditions close packing was achieved, leading to a continuous uniform film—see Fig. 9.

The electrostatically driven integration of ITO, **1** and Fe(II)Cyt*c* building blocks gave a device showing a functionality based on the redox protein.[22] Reversible switching between two well-defined states was attained by altering the redox state of the iron center. The application of different electrochemical potentials switched the photoperformance ON (Fe(II)Cyt*c*) or OFF (Fe(III)Cyt*c*)—see Fig. 10. A promising asset of this work is that stacking donor–acceptor sandwich layers (*i.e.*, Fe(III)Cyt*c*–**1**) helps to enhance the photosensitivity of the switch nearly linearly with the absorption cross section of the modified ITO electrodes.

In a more traditional dyad, in which C_{60} and the donor are covalently linked, the expected charge-flow—from the photoexcited chromophore to C_{60} and, finally to the semiconductor electrode—requires, for an optimum performance, the deposition of the C_{60} moiety onto the electrode. Therefore, the recognition motif (*i.e.*, a positively charged $-NH_3^+$ terminus) was placed onto the fullerene end, rather than locating it at the chromophore, such as in **7**. The free-base tetraphenylporphyrin or nickel(II) tetraphenylporphyrin-C_{60} donor–acceptor ensemble (*i.e.*, C_{60}–H_2P (**8**)[23] and C_{60}–NiP (**9**)[24] and a polyelectrolyte surface (*i.e.*, PSS) were deposited on photoactive ITO-electrodes, driven by simple electrostatic interactions. The photoaction spectra of the **8**- and **9**-sensitized semiconductor ITO electrodes reveal the free-base tetraphenylporphyrin or nickel(II) tetraphenylporphyrin moieties as the photoactive species with electrons migrating from the deposited films to the ITO electrode. In response to visible light irradiation, injection of electrons into the ITO conduction band occurred directly from the photochemically generated $C_{60}^{\bullet-}$–$H_2P^{\bullet+}$ or $C_{60}^{\bullet-}$–$NiP^{\bullet+}$ radical pairs and indirectly *via* electron transport

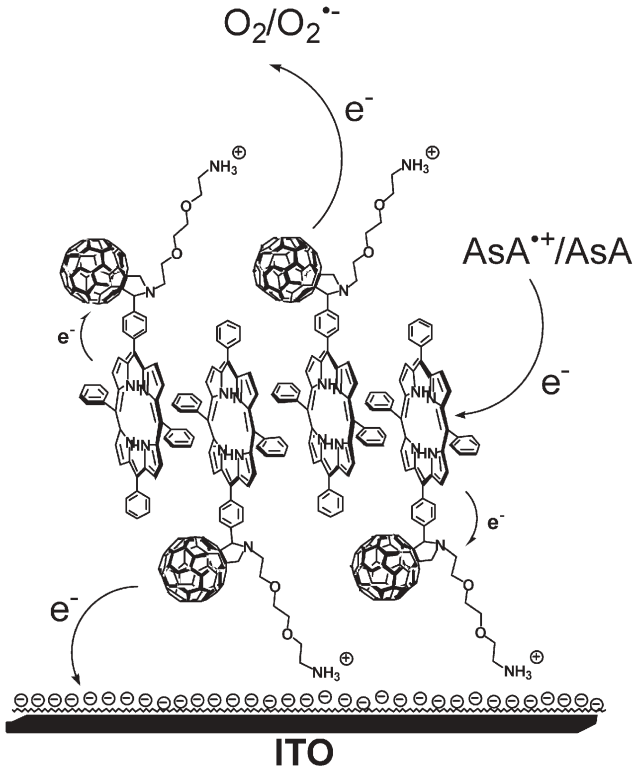

Fig. 11 Schematic illustration of photocurrent generation in ITO-electrodes covered with a single layer film of **8**.

mediated through suitable electron carriers (*i.e.*, O_2 and methylviologen). A schematic illustration is summarized in Fig. 11.

Photocurrents under monochromatic light illumination of the ITO/PDDA/PSS/**9** (IPCE 0.01%) are similar to those recorded for ITO/PDDA/PSS/**8**. Exact experimental conditions were 0.1 M NaH_2PO_4, 1 mM ascorbic acid and nitrogen. Replacement of 0.1 M NaH_2PO_4 with 0.1 M NaCl, while leaving 1 mM ascorbic acid and nitrogen, led to a 5-fold drop in photocurrent, indicating an enhanced surface activation.

Sequential repeated depositions of **8** or **9** and PSS allowed the systematic stacking of individual sandwich layers. However, photocurrents evolving from the efficient generation of charge-separated states showed only a moderate increase with the number of layers deposited. To improve the conductance between the aqueous environment and the ITO electrode and therefore to obtain higher efficiencies of the modified ITO-electrodes, we developed two alternative deposition strategies, namely: (i) application of long-range excited state and electron transfer gradients and (ii) replacement of the insulating PSS or PDDA matrices with single wall carbon nanotubes (SWNT).

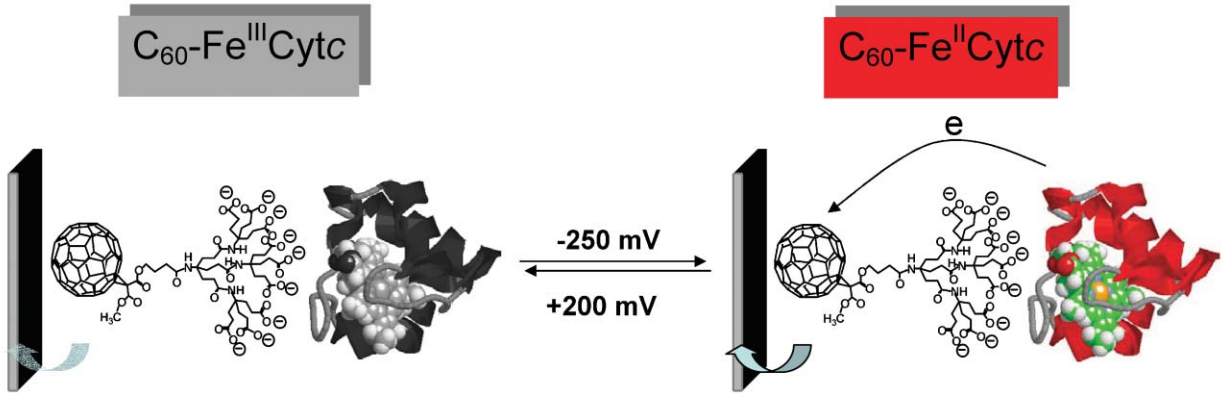

Fig. 10 Schematic illustration of electrochemical switching the redox protein-based construct between ON (Fe(II)Cyt*c*) and OFF (Fe(III)Cyt*c*) states.

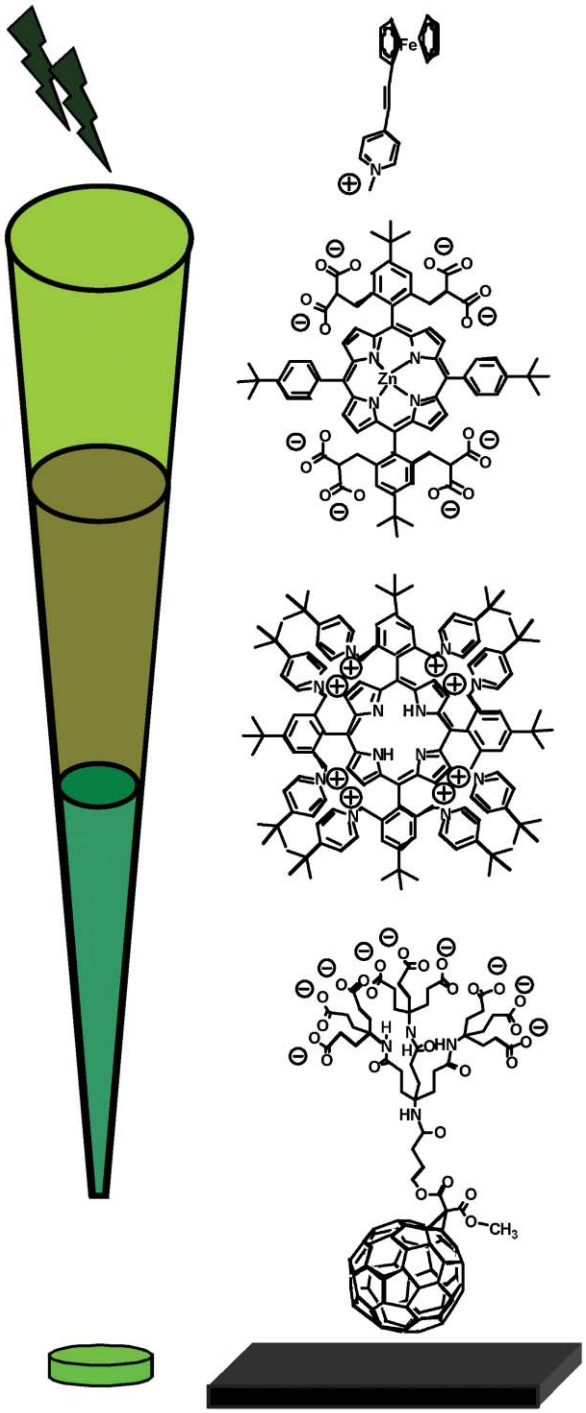

Fig. 12 Redox gradient in ITO, **1**, H_2P, ZnP, Fc.

Redox gradients

The advantage of packing the building blocks individually was used to generate a redox gradient along the deposition path illustrated in Fig. 12. These gradients are essential in helping (i) to attain good absorption coverage of the solar spectrum, (ii) to funnel solar light unidirectionally to an active core, (iii) to separate charges within that active core, and (iv) to transport electrons and holes into opposite directions.[25]

This approach differs from the above-discussed LBL strategy, where sandwich layers of covalently linked donor–acceptor dyads were integrated between layers of polyelectrolytes, but affording small IPCEs.

Following the controlled deposition of **1**, H_2P, ZnP, Fc building blocks—utilizing electrostatic and van der Waals interactions—ITO-electrodes were modified that showed remarkable IPCEs of up to 1.6%. Relative to the simplest systems (*i.e.*, PDDA/**1**), this corresponds to a 108-fold performance improvement.

The validity of the model redox gradient was easily verified by varying the order of deposition of the components. For example, an H_2P/**1** construct, instead of **1**/H_2P, showed a 5-fold drop in photocurrent. This is due to the mismatches in the individual redox steps: Instead of an electron injection evolving from $C_{60}^{\bullet-}$, the photocurrent mechanism must change to hole injection from the oxidized $H_2P^{\bullet+}$. To confirm this assumption and to overcome the resulting effects, an electrical bias to either accelerate or decelerate the charge injection into ITO was applied. For **1**/H_2P, going in 200 mV intervals from +200 mV to −400 mV, a gradual photocurrent decrease up to 54% was observed. This decrease reflects the fact that, parallel with the bias, the energy gap for $C_{60}^{\bullet-} \rightarrow ITO_{electron}$ is reduced and the flow of charges is suppressed. For H_2P/**1**, under the same conditions, 35% higher photocurrents are generated, suggesting that $H_2P^{\bullet+} \rightarrow ITO_{hole}$ becomes more and more exothermic. In a different experiment, aerobic and anaerobic conditions were compared and differences were found only for H_2P/**1**, which maximized at 20% photocurrent loss. In conclusion, photoexcitation of the porphyrin chromophores is succeeded by the formation of $C_{60}^{\bullet-}/H_2P^{\bullet+}$ or $C_{60}^{\bullet-}/ZnP^{\bullet+}$. From the reduced acceptor (*i.e.*, $C_{60}^{\bullet-}$) the electrons flow exothermically to the ITO conduction band. The oxidized donors (*i.e.*, $H_2P^{\bullet+}$ or $ZnP^{\bullet+}$), on the other hand, are reduced at the solid/liquid interface by ascorbate.

Carbon nanotubes

Single wall carbon nanotubes (SWNT)—Fig. 13—are suitable electron conducting materials, whose layers when interfacing **7**, **10**, **11**, *etc.* might improve the electron or energy storage features of the resulting device. The mechanical failure of hybrid materials made from polymers and SWNTs is primarily attributed to poor matrix/SWNT connectivity and severe phase segregation. Such problems can be successfully mitigated when the SWNT composite is made following the protocol of LBL assembly. This deposition technique prevents phase segregation of the polymer/SWNT binary system, and after subsequent cross-linking, the nm-scale-uniform composite with SWNT loading as high as 50 wt% can be obtained.[26]

SWNT can be easily oxidized, giving rise to carboxylic acid groups at the tips and sidewalls of the tubes. The presence of carboxylic acid functionalities allows the preparation of SWNT dispersions after 1 min sonication in deionized water without any additional surfactant. Thus prepared negatively charged SWNT were LBL assembled with positively charged polyelectrolyte, such as branched poly(ethyleneimine) (PEI). In every 5th deposition cycle, a layer of SWNT was replaced with a layer of poly(acrylic acid) (PAA) to improve the linearity of the deposition process.

The high structural homogeneity and interconnectivity of the structural components of the LBL films combined with high SWNT loading leads to significant increase of the strength of SWNT composites. In particular, free-standing SWNT/polyelectrolyte membranes delaminated from the substrate were

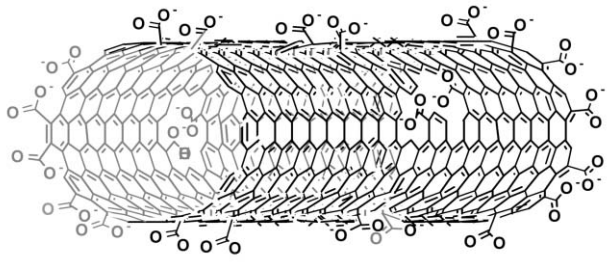

Fig. 13 Structure of negatively charged SWNT.

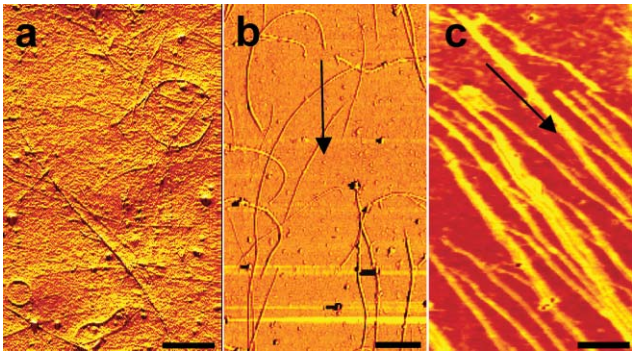

Fig. 14 Phase contrast AFM images of SWNT layers adsorbed to the polyelectrolyte monolayer in static conditions (a) and under laminar flow (b, c). The bars represent 400 nm (a, b) and 300 nm (c) and the arrows indicate the direction of the laminar flow.

found to be exceptionally strong with tensile strength approaching that of hard ceramics. Considering the light-weight nature of SWNT composites the prepared free-standing membranes can serve as unique components for a variety of long lifetime devices.

Depending on the deposition conditions, two types of SWNT organized structures were observed in polyelectrolyte adsorption films: self-assembled SWNT rings and flow-induced parallel ribbons.[27] The rings are likely to form directly on the surface of the polyelectrolyte-coated substrates because their substantial quantity would otherwise be observed in dense SWNT LBL films. Ring formation clearly indicates substantial mobility of the SWNT in the adsorption layer, which can also be seen in ring opening and has been utilized here for SWNT flow alignment—see Fig. 14. It is important to note that the parallel ribbons represent the first step to highly organized LBL multilayer composites with a specific orientation of the nanotubes in each layer leading to materials with mechanical, optical and electrical characteristics hard to achieve by other means including melt processing methods with polymers—poly(methyl methacrylate), *etc.*—or introduction of strong magnetic or electric fields.

In preliminary studies, which focused on comparing sets of ITO electrodes modified with SWNT/ZnP and PDDA/ZnP LBL systems, we confirmed the success of integrating SWNT. Not only that the photocurrents increased appreciably as a function of deposited SWNT and ZnP layers—even at 20 layers—but also that the photocurrents are magnitudes higher in the case of SWNT/ZnP.

Conclusions and outlook

Since their discovery C_{60} and SWNTs have attracted considerable attention due to their unique chemical and physical properties as well as their promise in the area of materials chemistry. For their full potential to be realized, compounds that are more compatible with composites and more soluble are to be generated. In this context, the current article highlights simple electrostatic interactions between suitably functionalized building blocks that gave original examples of molecular organization—from which unprecedented and useful nanostructures and nanomaterials evolve—and that might find application in the selected areas of nanoscience and nanotechnology. Importantly, a wide choice of inexpensive, durable, and readily synthesized device materials can produce unprecedented and useful nanostructures. These new materials can be utilized to achieve a more efficient way to convert the energy from sunlight into electricity.

The versatility of nanoparticle chemistry and LBL deposition process opens the exciting possibilities for further engineering the redox processes in homogeneous (*i.e.*, condensed media) and heterogeneous environments (*i.e.*, electrode surfaces). One of the areas of future research will be acceleration of the charge transport in the film by means of rationally designing multilayer stacks of NP with improved optical and electronic property gradients (such as absorption cross section in the visible region, fluorescence yields, redox features, *etc.*).

Equally intriguing is the concept to interface donor–acceptor structure with suitable electron conducting layers—organic and polymeric nanocomposite materials based on carbon nanotubes and semiconducting polymers—en route to systematic and uniform stacks of organized LBL nanoconstructs. As briefly mentioned, initial assays with poly-charged SWNTs reveal a particularly promising picture. We continue to study the fabrication of high quality, robust and photoactive ITO electrodes with fascinating and long-lasting solar energy conversion features.

Acknowledgements

This work was carried out with partial support from the EU (RTN network "WONDERFULL"), MIUR (PRIN 2002, prot. 2002032171), and the Office of Basic Energy Sciences of the US Department of Energy. This is document NDRL-4559 from the Notre Dame Radiation Laboratory. We are deeply indebted to our friends and collaborators Warren Ford, Andreas Hirsch, Norbert Jux, Nicholas A. Kotov, Michele Maggini, Lodovico Valli and Israel Zilbermann for their productive collaboration and numerous stimulating discussions.

Notes and references

1 (*a*) *Introduction to Nanotechnology*, ed. C. P. Poole and F. J. Owens, Wiley-Interscience, Weinheim, 2003; (*b*) *Nanophysics and Nanotechnology: An Introduction to Modern Concepts in Nanoscience*, ed. E. L. Wolf, John Wiley & Sons, New York, 2004.

2 (*a*) G. McDermott, S. M. Priece, A. A. Freer, A. M. Hawthornthwaite-Lawless, M. Z. Papiz, R. J. Cogdell and N. W. Isaacs, *Nature*, 1995, **374**, 517; (*b*) J. Barber, *Nature*, 1988, **333**, 114; (*c*) *Supramolecular Chemistry*, ed. V. Balzani and L. de Cola, NATO ASI Series; Kluwer Academic Publishers, Dordrech, 1992; (*d*) F. Vögtle, *Supramolecular Chemistry*, Wiley, Chichester, 1991; (*e*) J. M. Lehn, *Supramolecular Chemistry—Concepts and Perspectives*, VCH, Weinheim, 1995; (*f*) J. W. Steed and J. L. Atwood, *Supramolecular Chemistry*, Wiley, Chichester, 2000; (*g*) *Comprehensive Supramolecular Chemistry Vol. 1–10*, ed. J. L. Atwood, J. E. D. Davies, D. D. MacNicol, F. Vögtle and J.-M. Lehn, Pergamon/Elsevier, Oxford, UK, 1996; (*h*) L. F. Lindoy and I. M. Atkinson, *Self-Assembly in Supramolecular Systems*, Royal Society of Chemistry, Cambridge, UK, 2000; (*i*) *Nanoparticles and Nanostructured Films*, ed. J. H. Fendler, Wiley, Weinheim, 1998.

3 *Electron Transfer in Chemistry Vol. I–V*, ed. V. Balzani, Wiley-VCH, Weinheim, 2001.

4 (*a*) F. Diederich and R. Kessinger, *Acc. Chem. Res.*, 1999, **32**, 537; (*b*) *Fullerenes and Related Structures*, ed. A. Hirsch, *Top. Curr. Chem.*, Vol. 199, Springer, Berlin, 1999; (*c*) M. Prato and M. Maggini, *Acc. Chem. Res.*, 1998, **31**, 519; (*d*) *Lecture Notes on Fullerenes Chemistry*; ed. R. Taylor, Imperial College Press, London, 1999; (*e*) *Fullerenes: From Synthesis to Optoelectronic Properties*, ed. D. M. Guldi and N. Martín, Kluwer Academic Publishers, Dordrecht, 2002.

5 (*a*) *Carbon Nanotubes and Related Structures: New Materials for the Twenty-First Century*, Cambridge University Press, Cambridge, 2001; (*b*) *Carbon Nanotubes: Synthesis, Structure, Properties and Applications*, ed. M. S. Dresselhaus, G. Dresselhaus and P. Avouris, Springer, Berlin, 2001; (*c*) S. Reich, C. Thomsen and J. Maultzsch, *Carbon Nanotubes: Basic Concepts and Physical Properties*, VCH, Weinheim, 2004.

6 (*a*) H. Imahori and Y. Sakata, *Adv. Mater.*, 1997, **9**, 537; (*b*) M. Prato, *J. Mater. Chem.*, 1997, **7**, 1097; (*c*) N. Martin, L. Sanchez, B. Illescas and I. Perez, *Chem. Rev.*, 1998, **98**, 2527; (*d*) H. Imahori and Y. Sakata, *Eur. J. Org. Chem.*, 1999, 2445; (*e*) F. Diederich and M. Gomez-Lopez, *Chem. Soc. Rev.*, 1999, **28**, 263; (*f*) D. M. Guldi, *Chem. Commun.*, 2000, 321; (*g*) C. A. Reed and R. D. Bolskar, *Chem. Rev.*, 2000, **100**, 1075; (*h*) D. Gust, T. A. Moore and A. L. Moore, *J. Photochem. Photobiol. B*, 2000, **58**, 63; (*i*) D. Gust, T. A. Moore and A. L. Moore, *Acc. Chem. Res.*, 2001, **34**, 40; (*j*) D. M. Guldi and N. Martin, *J. Mater. Chem.*, 2002, **12**, 1978; (*k*) D. M. Guldi, *Chem. Soc. Rev.*, 2002, **31**, 22; (*l*) D. M. Guldi, T. Da Ros, P. Braiuca, M. Prato and E. Alessio, *J. Mater. Chem.*, 2002, **12**, 2001; (*m*) H. Imahori, Y. Mori and Y. Matano, *J. Photochem. Photobiol. C*, 2003, **4**, 51; (*n*) J. F. Nierengarten, *Top. Curr. Chem.*, 2003, **228**, 87; (*o*) D. M. Guldi, *Pure Appl. Chem.*, 2003, **75**,

1069; (*p*) M. E. El-Khouly, O. Ito and F. D'Souza, *J. Photochem. Photobiol. C*, 2004, **5**, 79.
7 *The Porphyrin Handbook*, ed. K. M. Kadish, K. M. Smith and R. Guilard, Academic Press, New York, 1999.
8 H. Imahori, D. M. Guldi, K. Tamaki, Y. Yoshida, C. Luo, Y. Sakata and S. Fukuzumi, *J. Am. Chem. Soc.*, 2001, **103**, 6617.
9 (*a*) G. Decher and J. D. Hong, *Ber.Bunsen-Ges.Phys.Chem.*, 1991, **95**, 1430; (*b*) M. Ferreira, J. H. Cheung and M. F. Rubner, *Thin Solid Films*, 1994, **244**, 806; (*c*) S. W. Keller, H. N. Kim and T. E. Mallouk, *J. Am. Chem. Soc.*, 1994, **116**, 8817; (*d*) Y. Lvov, G. Decher, H. Haas, H. Mohwald and A. Kalachev, *Physica B*, 1994, **198**, 89; (*e*) N. A. Kotov, *Nanostructured Mater.*, 1999, **12**, 789; (*f*) S. T. Dubas and J. B. Schlenoff, *Macromolecules*, 1999, **32**, 8153; (*g*) P. T. Hammond, *Curr. Opin. Colloid Interface Sci.*, 2000, **4**, 430; (*h*) M. F. Durstock, B. Taylor, R. J. Spry, L. Chiang, S. Reulbach, K. Heitfeld and J. W. Baur, *Synth. Metals*, 2001, 116; (*i*) M. Ferreira, M. F. Rubner and B. R. Hsieh, *MRS Symp. Proc.*, 1994, **328**, 119; (*j*) S. Yoo, S. S. Shiratori and M. F. Rubner, *Macromolecules*, 1998, **31**, 4309.
10 M. Brettreich and A. Hirsch, *Tetrahedron Lett.*, 1998, **39**, 2731.
11 (*a*) L. Echegoyen and L. E. Echegoyen, *Acc. Chem. Res.*, 1998, **31**, 593; (*b*) E. Dietel, A. Hirsch, J. Zhou and A. Rieker, *J. Chem. Soc. Perkin Trans. 2*, 1998, 1357; (*c*) X. Camps, E. Dietel, A. Hirsch, S. Pyo, L. Echegoyen, S. Hackbarth and B. Röder, *Chem. Eur. J.*, 1999, **5**, 2362.
12 D. M. Guldi and M. Prato, *Acc. Chem. Res.*, 2000, **33**, 695.
13 D. Balbinot, S. Atalick, D. M. Guldi, M. Hatzimarinaki, A. Hirsch and N. Jux, *J. Phys. Chem.*, 2003, **107**, 13273.
14 M. Braun, S. Atalick, D. M. Guldi, H. Lanig, M. Brettreich, S. Burghardt, M. Hatzimarinaki, E. Ravanelli, R. van Eldik and A. Hirsch, *Chem. Eur. J.*, 2003, **9**, 3867.
15 (*a*) D. M. Guldi, M. Marcaccio, D. Paolucci, F. Paolucci, N. Tagmatarchis, D. Tasis, E. Vázquez and M. Prato, *Angew. Chem., Int. Ed.*, 2003, **42**, 4206; (*b*) M. Melle-Franco, M. Marcaccio, D. Paolucci, F. Paolucci, V. Georgakilas, D. M. Guldi, M. Prato and F. Zerbetto, *J. Am. Chem. Soc.*, 2004, **126**, 1646.
16 S. Qin, D. Qin, W. T. Ford, J. E. Herrera, D. E. Resasco, S. M. Bachilo and R. B. Weisman, *Macromolecules*, 2004, **37**, 3965.
17 D. M. Guldi, G. M. A. Rahman, J. Ramey, M. Marcaccio, D. Paolucci, F. Paolucci, S. Qin, W. T. Ford, D. Balbinot, N. Jux, N. Tagmatarchis and M. Prato, *Chem. Commun.*, 2004, 2034.
18 D. M. Guldi, I. Zilbermann, G. A. Anderson, N. A. Kotov and M. Prato, *J. Am. Chem. Soc.*, 2004 in press.
19 L. Valli and D. M. Guldi, in *Fullerenes: From Synthesis to Optoelectronic Properties*, eds. D.M. Guldi and N. Martín, Kluwer Academic Publishers, Dordrecht, 2002.
20 (*a*) S. Conoci, D. M. Guldi, S. Nardis, R. Paolesse, M. Prato, G. Ricciardi, G. M. H. Vicente, L. Valli and I. Zilbermann, *Chem. Eur. J.*, 2004 in press; (*b*) A. P. Maierhofer, M. Brettreich, S. Burghardt, O. Vostrowsky, A. Hirsch, S. Langridge and T. M. Bayerl, *Langmuir*, 2000, **16**, 8884.
21 (*a*) C. Luo, D. M. Guldi, M. Maggini, E. Menna, S. Mondini, N. A. Kotov and M. Prato, *Angew. Chemie, Int. Ed.*, 2000, **39**, 3905; (*b*) D. M. Guldi, M. Maggini, F. Paolucci and S. Hotchandani, *Fuller. Nanotub. Carb. N.*, 2003, **11**, 121; (*c*) D. M. Guldi, in *Nanoparticles in Solids and Solutions*, ed. J. H. Fendler, VCH Weinheim; New York, 1998.
22 D. M. Guldi, I. Zilbermann, A. Lin, M. Braun and A. Hirsch, *Chem. Commun.*, 2004, 96.
23 D. M. Guldi, F. Pellarini, M. Prato, C. Granito and L. Troisi, *Nano Lett.*, 2002, **2**, 965.
24 D. M. Guldi, I. Zilbermann, G. A. Anderson, K. Kordatos, M. Prato, R. Tafuro and L. Valli, *J. Mater. Chem.*, 2004, **14**, 303.
25 D. M. Guldi, I. Zilbermann, G. A. Anderson, A. Li, D. Balbinot, N. Jux, M. Hatzimarinaki, A. Hirsch and M. Prato, *Chem. Commun.*, 2004, 726.
26 A. A. Mamedov, N. A. Kotov, M. Prato, D. M. Guldi, J. P. Wicksted and A. Hirsch, *Nat. Mater.*, 2002, **1**, 190.
27 D. M. Guldi, N. Kotov, A. Hirsch and M. Prato, *J. Phys. Chem. B*, 2004, **108**, 8770.